

25. Xirodimas, D., Saville, M. K., Bourdon, J. C., Hay, R. T. & Lane, D. P. Mdm2-mediated NEDD8 conjugation of p53 inhibits its transcriptional activity. *Cell* **118**, 83–97 (2004).
26. Cutler, R. G. *et al.* Involvement of oxidative stress-induced abnormalities in ceramide and cholesterol metabolism in brain aging and Alzheimer's disease. *Proc. Natl Acad. Sci. USA* **101**, 2070–2075 (2004).
27. Thompson, J. D., Higgins, D. G. & Gibson, T. J. CLUSTAL W: improving the sensitivity of progressive multiple sequence alignment through sequence weighting, position-specific gap penalties and weight matrix choice. *Nucleic Acids Res.* **22**, 4673–4680 (1994).

Supplementary Information accompanies the paper on www.nature.com/nature.

Acknowledgements We thank R. Weinberg for pWZLhygro-TERT, R. Bernards for pSUPER, and D. Shalloway and J. L. Bos for GST-RBD. A. Osborn and M. Tetzlaff are thanked for help with Seladin-1 cDNA colony hybridization and early construct preparations. M. Serrano is thanked for *INK4a/ARF* knockout and control MEFs. We also thank L. Donehower for discussions and A. Beaudet for continuing support of this project. This work was supported in part by grants from US DOD and the Gustav and Louise Pfeiffer Research Foundation (K.G.) and AIRC (Italian Association for Cancer Research, R.M.).

Competing interests statement The authors declare that they have no competing financial interests.

Correspondence and requests for materials should be addressed to K.G. (kgalakt@bcm.tmc.edu).

Poly(ADP-ribose) is required for spindle assembly and structure

Paul Chang¹, Myron K. Jacobson² & Timothy J. Mitchison¹

¹Department of Systems Biology, Harvard Medical School, Boston, Massachusetts 02115, USA

²Department of Pharmacology and Toxicology, College of Pharmacy, and Arizona Cancer Center, University of Arizona, Tucson, Arizona 85721, USA

The mitotic spindle is typically thought of as an array of microtubules, microtubule-associated proteins and motors that self-organizes to align and segregate chromosomes¹. The major spindle components consist of proteins and DNA, the primary structural elements of the spindle¹. Other macromolecules including RNA and lipids also associate with spindles, but their spindle function, if any, is unknown. Poly(ADP-ribose) (PAR) is a large, branched, negatively charged polymeric macromolecule whose polymerization onto acceptor proteins is catalysed by a family of poly(ADP-ribose) polymerases (PARPs)². Several PARPs localize to the spindle in vertebrate cells, suggesting that PARPs and/or PAR have a role in spindle function². Here we show that PAR is enriched in the spindle and is required for spindle function—PAR hydrolysis or perturbation leads to rapid disruption of spindle structure, and hydrolysis during spindle assembly blocks the formation of bipolar spindles. PAR exhibits localization dynamics that differ from known spindle proteins and are consistent with a low rate of turnover in the spindle. Thus, PAR is a non-proteinaceous, non-chromosomal component of the spindle required for bipolar spindle assembly and function.

PAR polymers are the product of post-translational modifications and are required for normal cell division; in *Drosophila*, PARP knockouts are embryonic lethal³. PAR is polymerized by PARPs onto acceptor proteins using NAD⁺ as substrate², and the concentration, length and extent of PAR branching are regulated by a balance of activities of the PARPs and poly(ADP-ribose) glycohydrolase (PARG), a highly specific, processive endo- and exoglycosidase⁴. Most PARPs localize to the spindle: PARP1 and PARP2 localize to centromeres and interact with CENPA, CENPB and Bub3 (ref. 5); VPARP localizes throughout the spindle⁶; PARP1 and PARP3 associate with centrosomes²; and tankyrase1 and 2 are found at chromosomes and spindle poles⁷, where they interact with the spindle pole protein NuMA⁸. Cellular PAR concentrations

markedly increase during metaphase and anaphase–telophase owing to PARP activity⁹. Together, these observations suggest that PARPs, or PAR itself, might be important in spindle function.

We examined PAR localization in metaphase spindles by staining isolated spindles— assembled in cycled *Xenopus* egg extract and in somatic cells—using three different antibodies against PAR, and varied fixation conditions (Fig. 1a, b). In all cases, PAR was filamentous and punctate in appearance, co-localized with spindle microtubules, and was enriched at spindle poles and kinetochores (Fig. 1a, b; see also Supplementary Fig. S1). PAR filaments were most evident without fixation and became more punctate after fixation, suggesting that traditional fixation methods developed for proteins perturb PAR localization. PAR localization to the kinetochore is particularly interesting in light of data demonstrating PARP1 recruitment to metaphase centromeres¹⁰, suggesting a role for PARP1 or PAR in centromere/kinetochore function.

The staining pattern in metaphase cells was similar to isolated *Xenopus* spindles except for a more pronounced enrichment at the poles (Fig. 1b). At the poles, PAR was primarily associated with spindle pole material rather than centrosomes, and spindle pole staining was similar to the localization pattern seen for tankyrase1 (ref. 11). Interestingly, PARG also co-localized with spindle microtubules in BSC1 and HeLa cells (Fig. 1c). This co-localization of PARPs, PAR and PARG with spindle microtubules suggests that one or more PARP(s) and PARG may actively regulate PAR levels in the spindle.

To determine whether PAR is enriched in the metaphase spindle, we compared the amount of spindle-associated PAR to total mitotic frog egg extract (CSF) by isolating spindles from *Xenopus* extract, and resolving equivalent concentrations of purified spindles and CSF on SDS polyacrylamide gels. Immunoblotting with anti-PAR antibodies showed a ~10-fold enrichment of PAR in the spindle relative to surrounding cytoplasm (Figs 1d and 2c). Most of the poly(ADP-ribosyl)ated (PARsylated) proteins were between ~97 and ~200 kDa. These may represent a single, highly modified protein, or a population of PARsylated proteins of varying sizes (Figs 1d and 2c). PAR and tubulin concentrations were unaffected by detergent treatment before spindle isolation, showing that PAR directly associates with the spindle rather than the membranes that co-purify with isolated spindles.

To ask whether PAR has an important function in the spindle, we assembled spindles in the presence of X-rhodamine-labelled tubulin in extracts containing replicated chromosomes¹² (cycled spindles), and perturbed PAR polymer by adding exogenous PARG or high concentrations of purified anti-PAR antibodies. We observed spindle structure using real-time, spinning-disk confocal microscopy (Fig. 2a) or examined fixed samples at defined time points (Fig. 2b, e). Notably, addition of 100 µg ml⁻¹ PARG resulted in the rapid breakdown of spindle structure (Fig. 2a; see also Supplementary Movie M1). Microtubules rapidly splayed outward from the spindle centre, after which the two half spindles appeared to become disconnected and the degree of anti-parallel microtubule overlap decreased markedly. This effect was specific to the hydrolytic activity of PARG, as simultaneous addition of 100 µM of the PARG inhibitor ADP-HPD¹³ blocked the phenotypic effect of PARG (Fig. 2b). We quantified the effect of PARG addition on both PAR and tubulin concentrations in the spindle by isolating treated and untreated spindles and blotting for PAR or tubulin (Fig. 2c). Addition of 100 µg ml⁻¹ PARG to assembled spindle reactions resulted in the complete hydrolysis of PAR polymer up to the detection limit of our testing, whereas simultaneous addition of 100 µM ADP-HPD partially protected PAR, especially at high molecular weight. Addition of 500 µg ml⁻¹ of affinity-purified anti-PAR antibody to cycled spindles phenocopied the effects of PARG addition (Fig. 2a; see also Supplementary Movie M2). In all cases extracts remained in mitosis, as demonstrated by the presence of condensed chromosomes. The phenotype of PAR hydrolysis was not

due to increased concentrations of soluble PAR, as addition of $500 \mu\text{g ml}^{-1}$ purified exogenous PAR had no effect on spindle structure (not shown). Taken together, these results suggest that PAR within the spindle is required for maintenance of bipolar spindle structure.

To determine whether PAR is required for the assembly of spindles, we added PARG before spindle assembly and analysed fixed samples 30 min after bipolar spindles had formed in untreated control reactions. Addition of $100 \mu\text{g ml}^{-1}$ PARG led to a complete

abrogation of spindle assembly—no bipolar spindles were identified in ten fields analysed at $40\times$ magnification. However, monopolar microtubule asters were present in association with normal mitotic chromosomes (Fig. 2b). Co-incubation of PARG and $100 \mu\text{M}$ ADP-HPD partially restored spindle assembly (Fig. 2b)—60 bipolar spindles were identified in ten random fields in two independent experiments. The presence of microtubule asters suggests that PAR is specifically required for bipolar spindle assembly. Furthermore, when we treated non-chromosomal, acen-

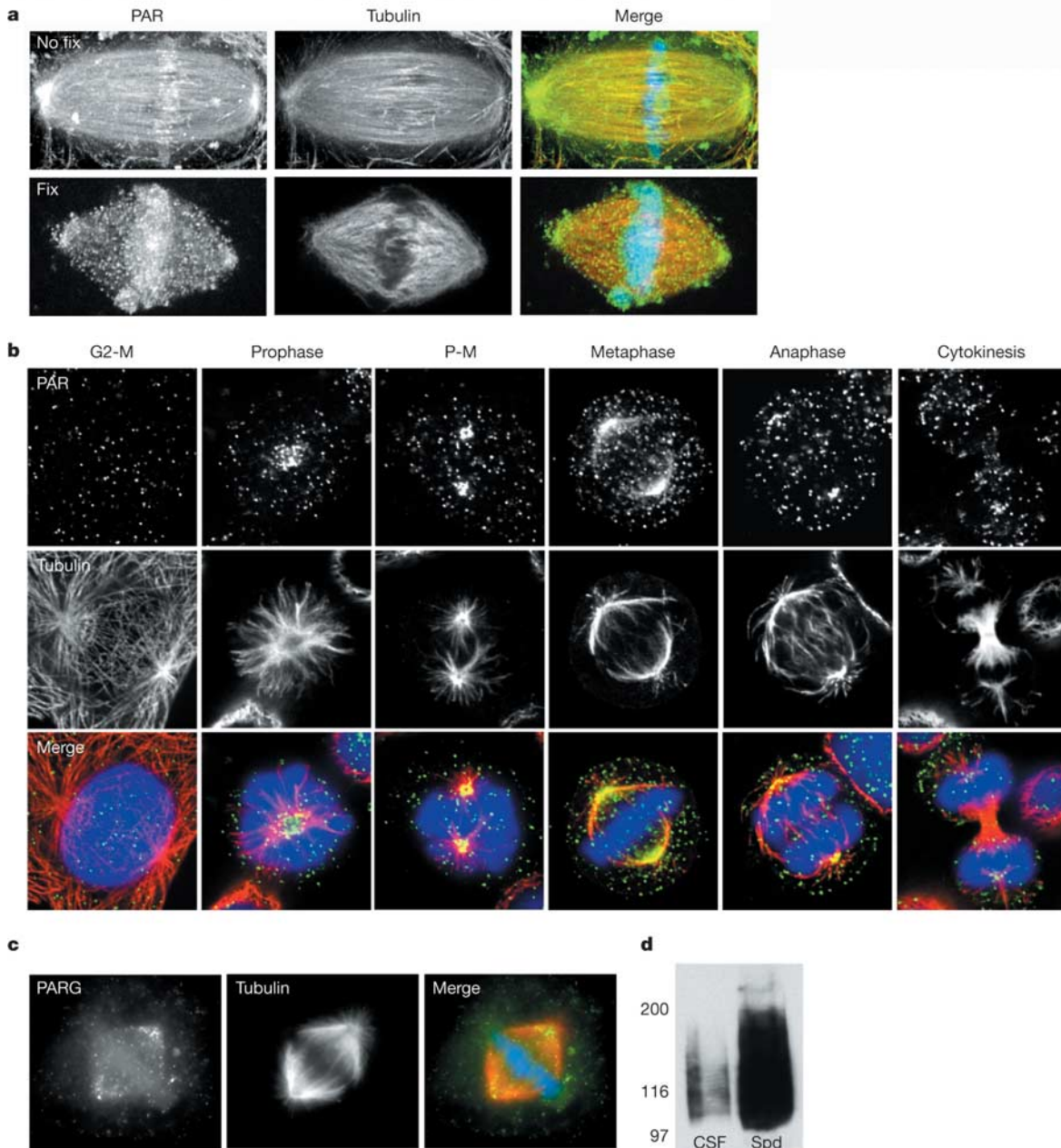


Figure 1 PAR is enriched in the spindle. **a**, PAR localization in purified *Xenopus* spindles. *Xenopus* egg extract spindles were isolated and stained for PAR, tubulin and DNA, without fixation (no fix), or after fixing with 4% paraformaldehyde (fix). PAR localizes throughout the spindle and is enriched at kinetochores and spindle poles (Supplementary Fig. S1). PAR appears filamentous when not fixed, and appears more punctate after fixation. In the merged panel, PAR is green, tubulin red and DNA is blue. **b**, Mitotic localization of PAR in somatic cells. HeLa, U2OS, LLPCK, XLK and BSC1 cells were fixed and stained for PAR, tubulin and DNA. All cell types exhibited similar staining patterns. HeLa cells during G2-M, prophase, prometaphase (P-M), metaphase, anaphase and cytokinesis stages of the cell

cycle are shown. PAR localizes to the mitotic spindle throughout mitosis and appears filamentous during metaphase, similar to the staining pattern seen in isolated *Xenopus* egg extract spindles, which are arrested in metaphase. In the merged panel, PAR is green, tubulin red and DNA is blue. **c**, PARG localizes to the mitotic spindle. HeLa cells were stained with antibodies against PARG and tubulin. PARG co-localizes with tubulin, as shown in the merged panel (PARG is green, tubulin red and DNA is blue). **d**, PAR is enriched in the spindle. Immunoblot of equivalent amounts of CSF extract or isolated spindles (Spd) probed with anti-PAR antibody. Molecular mass is marked along the left (kDa).

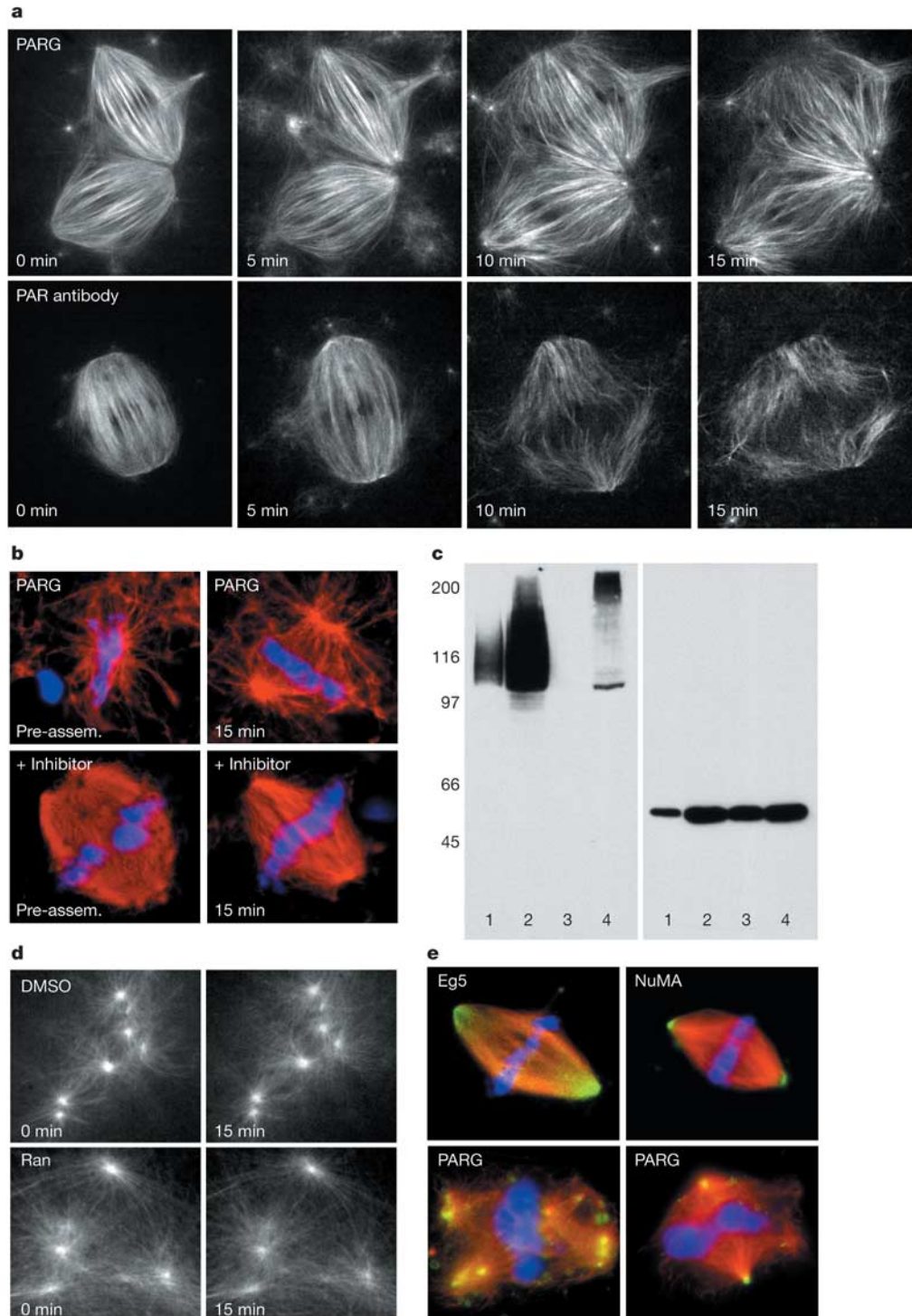


Figure 2 PAR is required for bipolar spindle assembly and function. **a**, PAR perturbation results in rapid loss of spindle structure. Cycled *Xenopus* egg extract spindles assembled in the presence of X-rhodamine-labelled tubulin were treated with $100 \mu\text{g ml}^{-1}$ PARG or $500 \mu\text{g ml}^{-1}$ purified anti-PAR antibody, and real-time images obtained every 30 s for 15 min on a spinning disk microscope. (See Supplementary Movie M1 (PARG addition) and Supplementary Movie M2 (PAR antibody addition) for full sequences.) **b**, PAR is required for spindle assembly and function. Addition of $100 \mu\text{g ml}^{-1}$ PARG for 2 h during (pre-assem.) and for 15 min after (15 min) spindle assembly both resulted in spindle monopoles with associated condensed chromosomes. These phenotypes are specific for PAR hydrolysis, as addition of $100 \mu\text{M}$ ADP-HPD (+inhibitor), a PARG inhibitor, rescues spindle bipolarity. Tubulin is red and DNA is blue. **c**, Quantification of PAR hydrolysis. Equal amounts of CSF extract (lane 1) or cycled spindles reactions were untreated (lane 2),

treated with $100 \mu\text{g ml}^{-1}$ PARG (lane 3), or $100 \mu\text{g ml}^{-1}$ PARG plus $100 \mu\text{M}$ ADP-HPD (lane 4) and probed for antibodies against PAR (left blot) or tubulin (right blot). PARG treatment (lane 3) results in complete hydrolysis of PAR, whereas simultaneous addition of ADP-HPD partially protected PAR (lane 4). Molecular mass is indicated along the left (kDa). **d**, PAR is not required for microtubule aster structure or assembly. A total of $100 \mu\text{g ml}^{-1}$ PARG was added 25 min before DMSO- or RanGTP-induced (Ran) aster assembly in CSF extract, and real-time images obtained every 30 s for 15 min. PARG addition had no effect on aster assembly or structure. **e**, Eg5 and NuMA localization after PAR disruption. Cycled *Xenopus* extract spindles were not treated (top) or were treated with $100 \mu\text{g ml}^{-1}$ PARG (bottom), isolated and stained for tubulin (red) and Eg5 or NuMA (green), two proteins required for spindle assembly. Eg5 and NuMA remained associated with the resulting structures (PARG), suggesting that PAR may not be required for their targeting to spindles.

trosomal asters—formed by addition of Ran-GTP¹⁴ or DMSO—with 100 $\mu\text{g ml}^{-1}$ PARG (Fig. 2d), neither the size nor the density of asters was affected. Thus, PAR has a specific role in organizing bipolar spindles, and is not required for microtubule nucleation or dynamics.

We next determined the effect of PAR disruption on the localization of proteins previously implicated in spindle assembly: that is, Eg5, a tetrameric kinesin motor protein required for spindle bipolarity¹⁵, and NuMA, a non-centrosomal component of the spindle poles required for pole focusing¹⁶. Importantly, Eg5 (ref. 15) and NuMA¹⁷ localize to both bipolar spindles and microtubule asters. We added 100 $\mu\text{g ml}^{-1}$ PARG to assembled cycled spindles containing X-rhodamine-labelled tubulin, purified the resulting structures through glycerol cushions, and stained for Eg5 or NuMA (Fig. 2e). Both proteins associated with the microtubule structures, suggesting that PAR is not required for their

targeting to spindles, although we cannot rule out more subtle interactions of these proteins with PAR.

Microtubule-associated spindle components including tubulin, microtubule-associated proteins and Eg5 have been shown to exchange rapidly between spindle-associated and cytoplasmic pools^{18–20}. PAR differs biochemically and biophysically from known spindle molecules and might exhibit unique localization dynamics. As a first approach to analysing dynamics, we measured the half-life of anti-PAR Fab fragments bound to spindles. Fab fragments generated from purified anti-PAR LP96-10 antibody were directly labelled with X-rhodamine. In addition, we directly labelled LP96-10 IgG and anti-PAR IgY with X-rhodamine and Alexa 488. All yielded similar localization patterns. Directly labelled anti-PAR Fab was added to cycled spindles, and its localization examined using real-time wide-field microscopy (Fig. 3a). These low concentrations of antibody, unlike the 50 \times higher concentrations used earlier to disrupt spindle function, had no obvious effect on spindle morphology. To measure exchange between spindle-associated and cytoplasmic PAR, we concentrated spindles labelled with 10 $\mu\text{g ml}^{-1}$ X-rhodamine-labelled anti-PAR Fab by sedimentation, diluted them 1:20 in unlabelled extract, and measured the loss of fluorescence intensity relative to the initial time point. For comparison, we repeated the experiment using 10 $\mu\text{g ml}^{-1}$ X-rhodamine-labelled antibody against the microtubule-associated protein TPX2 (ref. 21). Labelled tubulin exchanged out of the spindle rapidly, as expected (not shown). TPX2 antibody exchanged out with a half-life of ~ 5 min, confirming that TPX2 is a dynamic spindle component. In contrast, PAR fluorescence did not decrease appreciably during the course of the dilution experiment (Fig. 3b), indicating a half-life longer than that of known spindle components.

Our data demonstrate a requirement for PAR in the assembly and structure of bipolar spindles, and help to explain PARP localization to the spindle. How might PAR function in the spindle? The best understood mechanism of PAR activity is regulation of polynucleosome activity during DNA damage: PARsylation of histones results in a conformational change in the polynucleosome leading to altered nucleosome–DNA interactions and changes in chromatin condensation²². Similarly, PARsylation of spindle proteins including microtubule-associated proteins and molecular motors may regulate their activity, and as a result, spindle assembly and function. Thus PAR may act as a molecular on/off ‘switch’ for spindle assembly. Phosphorylation, a hallmark of mitosis, increases the activity of PARP1 and tankyrase1 (refs 23, 24) and may regulate the activity of all PARPs. For example, PARP1 is inactive in oocytes, and PAR is not detectable; however, PARP activity is increased after phosphorylation of PARP1 by mitotic kinases, without any change in PARP protein concentrations²³. This suggests that phosphorylation may also regulate PARP activity during mitosis, explaining the increase in PAR concentration during mitosis⁹. We do not know the identity of PAR acceptors in the spindle aside from the PARPs themselves, as all known PARPs undergo auto(ADP-ribosylation). One interesting candidate is NuMA, a spindle protein required for spindle pole assembly and recently shown to interact directly with tankyrase1 (ref. 8). PARsylation of NuMA may be required for spindle function.

Another possibility is that PAR has a structural role in the spindle. The size, branching, high negative charge and aromatic heterocycle functionality of PAR suggest that it could mediate charge–charge interactions with proteins in addition to covalent modification of acceptors. This would explain the disruption of spindle structure observed when large amounts of anti-PAR antibody are added. PARsylated proteins in the nucleus have been shown to interact with non-modified proteins through charge–charge interactions with PAR, interactions thought to mediate assembly of a nuclear matrix²⁵. A similar matrix may exist in the spindle, as proposed by the spindle matrix hypothesis²⁶. Finally, we note that PARP1 is a

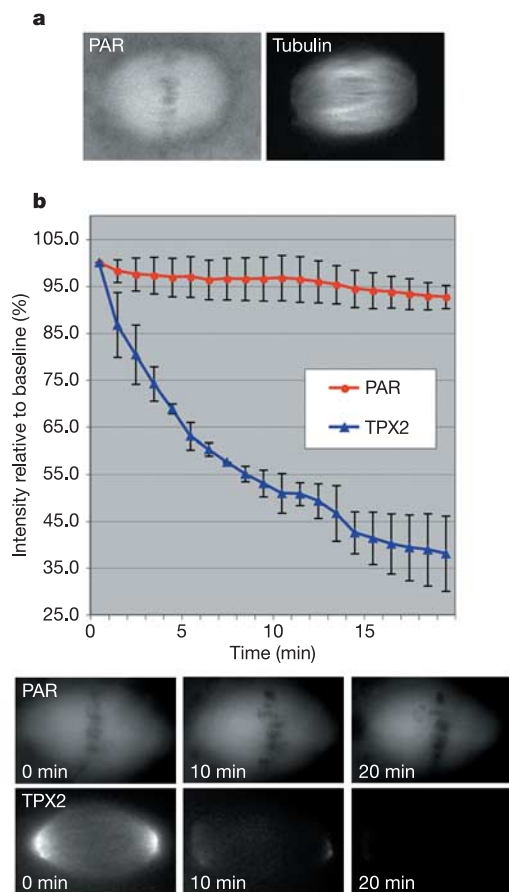


Figure 3 PAR exchange between the spindle and cytoplasm is slow. **a**, Real-time localization of PAR in the spindle. X-rhodamine-labelled anti-PAR Fab fragments were added to cycled spindles containing Alexa-488-labelled tubulin and visualized. PAR localization to the spindle largely overlaps with tubulin. **b**, Rate of PAR exchange between the spindle and cytoplasm. *Xenopus* egg extract spindles incubated with X-rhodamine-labelled anti-PAR Fab or anti-TPX2 antibodies were partially purified by sedimentation, diluted 1:20 into unlabelled mitotic egg extract and images taken every 30 s for 20 min using wide-field microscopy. The graph depicts the percentage relative fluorescence intensity with respect to time 0 at every minute for three separate experiments. PAR (red line) exhibits a slow rate of cytoplasmic exchange relative to TPX2 (blue line), longer than known spindle components. Error bars represent standard deviation of three independent experiments. Below are images of anti-PAR and anti-TPX2 antibodies at 0, 10 and 20 min.

common drug target²⁷, suggesting that the spindle-associated PARPs are potential cancer drug targets. □

Methods

Imaging and antibodies

Cycled *Xenopus* egg extract spindles were assembled as described¹² with or without X-rhodamine-labelled or Alexa-488-labelled tubulin, and isolated through 40% glycerol BRB80. For staining of non-fixed spindles, isolated spindles were processed for immunofluorescence in solutions containing 5% glycerol BRB80. For immunofluorescence and immunoblotting, polyclonal rabbit LP96-10 IgG was purchased from BD Biosciences, polyclonal chicken IgY anti-PAR antibodies from Tulip Biolabs, and monoclonal 10H from Trevigen. All anti-PAR antibodies were pre-adsorbed against BSA transferred to nitrocellulose. LP96-10 Fab fragments were generated using an Immunopure Fab preparation kit (Pierce Biotech). Anti-NuMA, TPX2 and Eg5 polyclonal rabbit antibodies were gifts from A. Groen and D. Miyamoto. Rabbit anti-PARG antibody was obtained from Oncogene Inc. Primary antibodies were directly labelled using Alexa 488 and X-rhodamine NHS esters (Molecular Probes) as per the manufacturer's instructions. Measurements of fluorescence intensity were calculated by background subtraction, then integration of fluorescence. Images were obtained using a Princeton Instruments CCD camera, controlled by Metamorph software (Universal Imaging Corp.). Spinning disk confocal microscopy movies were obtained using a Nikon TE2000U inverted microscope, a Perkin Elmer Ultraview spinning disk confocal head, and a Hamamatsu Orca ER cooled-CCD camera controlled using Metamorph software. Spindle reactions were imaged in open chambers²⁸, and images obtained every 30 s for 15 min.

Protein purification and biochemistry

Recombinant bovine PARG was expressed and purified as described²⁹. For quantification of PAR after PARG treatment, spindles treated with 100 µg ml⁻¹ PARG, 100 µg ml⁻¹ PARG plus 100 µM ADP-HPD, or untreated spindles were isolated as above and resolved on 8% SDS-PAGE gels, transferred to nitrocellulose, and probed with LP96-10 antibody. CSF was added for comparison.

Received 23 April; accepted 21 September 2004; doi:10.1038/nature03061.

1. Wittmann, T., Hyman, A. & Desai, A. The spindle: a dynamic assembly of microtubules and motors. *Nature Cell Biol.* **3**, E28–E34 (2001).
2. Smith, S. The world according to PARG. *Trends Biochem. Sci.* **26**, 174–179 (2001).
3. Tulin, A., Stewart, D. & Spradling, A. C. The *Drosophila* heterochromatic gene encoding poly(ADP-ribose) polymerase (PARG) is required to modulate chromatin structure during development. *Genes Dev.* **16**, 2108–2119 (2002).
4. Hatakeyama, K., Nemoto, Y., Ueda, K. & Hayaishi, O. Purification and characterization of poly(ADP-ribose) glycohydrolase. Different modes of action on large and small poly(ADP-ribose). *J. Biol. Chem.* **261**, 14902–14911 (1986).
5. Saxena, A., Saffery, R., Wong, L. H., Kalitsis, P. & Choo, K. H. Centromere proteins Cenpa, Cenpb, and Bub3 interact with poly(ADP-ribose) polymerase-1 protein and are poly(ADP-ribosyl)ated. *J. Biol. Chem.* **277**, 26921–26926 (2002).
6. Kickhoefer, V. A. et al. The 193-kD vault protein, VPARG, is a novel poly(ADP-ribose) polymerase. *J. Cell Biol.* **146**, 917–928 (1999).
7. Smith, S. & de Lange, T. Tankyrase promotes telomere elongation in human cells. *Curr. Biol.* **10**, 1299–1302 (2000).
8. Sbodio, J. I. & Chi, N. W. Identification of a tankyrase-binding motif shared by IRAP, TAB182, and human TRF1 but not mouse TRF1. NuMA contains this RXXPDG motif and is a novel tankyrase partner. *J. Biol. Chem.* **277**, 31887–31892 (2002).
9. Bakondi, E. et al. Detection of poly(ADP-ribose) polymerase activation in oxidatively stressed cells and tissues using biotinylated NAD substrate. *J. Histochem. Cytochem.* **50**, 91–98 (2002).
10. Earle, E. et al. Poly(ADP-ribose) polymerase at active centromeres and neocentromeres at metaphase. *Hum. Mol. Genet.* **9**, 187–194 (2000).
11. Smith, S. & de Lange, T. Cell cycle dependent localization of the telomeric PARG, tankyrase, to nuclear pore complexes and centrosomes. *J. Cell Sci.* **112**, 3649–3656 (1999).
12. Sawin, K. E. & Mitchison, T. J. Mitotic spindle assembly by two different pathways *in vitro*. *J. Cell Biol.* **112**, 925–940 (1991).
13. Slama, J. T. et al. Specific inhibition of poly(ADP-ribose) glycohydrolase by adenosine diphosphate (hydroxymethyl)pyrrolidinediol. *J. Med. Chem.* **38**, 389–393 (1995).
14. Wilde, A. & Zheng, Y. Stimulation of microtubule aster formation and spindle assembly by the small GTPase Ran. *Science* **284**, 1359–1362 (1999).
15. Sawin, K. E., LeGuellec, K., Philippe, M. & Mitchison, T. J. Mitotic spindle organization by a plus-end-directed microtubule motor. *Nature* **359**, 540–543 (1992).
16. Compton, D. A., Szilak, I. & Cleveland, D. W. Primary structure of NuMA, an intranuclear protein that defines a novel pathway for segregation of proteins at mitosis. *J. Cell Biol.* **116**, 1395–1408 (1992).
17. Dionne, M. A., Howard, L. & Compton, D. A. NuMA is a component of an insoluble matrix at mitotic spindle poles. *Cell Motil. Cytoskel.* **42**, 189–203 (1999).
18. Olmsted, J. B., Stemple, D. L., Saxton, W. M., Neighbors, B. W. & McIntosh, J. R. Cell cycle-dependent changes in the dynamics of MAP2 and MAP4 in cultured cells. *J. Cell Biol.* **109**, 211–223 (1989).
19. Kapoor, T. M. & Mitchison, T. J. Eg5 is static in bipolar spindles relative to tubulin: evidence for a static spindle matrix. *J. Cell Biol.* **154**, 1125–1133 (2001).
20. Saxton, W. M. et al. Tubulin dynamics in cultured mammalian cells. *J. Cell Biol.* **99**, 2175–2186 (1984).
21. Wittmann, T., Wilm, M., Karsenti, E. & Vernos, I. TPX2, A novel *Xenopus* MAP involved in spindle pole organization. *J. Cell Biol.* **149**, 1405–1418 (2000).
22. Poirier, G. G., de Murcia, G., Jongstra-Bilen, J., Niedergang, C. & Mandel, P. Poly(ADP-ribosylation) of polynucleosomes causes relaxation of chromatin structure. *Proc. Natl Acad. Sci. USA* **79**, 3423–3427 (1982).
23. Aoufouchi, S. & Shall, S. Regulation by phosphorylation of *Xenopus laevis* poly(ADP-ribose) polymerase enzyme activity during oocyte maturation. *Biochem. J.* **325**, 543–551 (1997).

24. Chi, N. W. & Lodish, H. F. Tankyrase is a golgi-associated mitogen-activated protein kinase substrate that interacts with IRAP in GLUT4 vesicles. *J. Biol. Chem.* **275**, 38437–38444 (2000).
25. Rouleau, M., Aubin, R. A. & Poirier, G. G. Poly(ADP-ribosyl)ated chromatin domains: access granted. *J. Cell Sci.* **117**, 815–825 (2004).
26. Pickett-Heaps, J. D., Forer, A. & Spurck, T. Traction fibre: toward a “tensegral” model of the spindle. *Cell Motil. Cytoskel.* **37**, 1–6 (1997).
27. Troll, W., Garte, S. & Frenkel, K. Suppression of tumor promotion by inhibitors of poly(ADP)ribose formation. *Basic Life Sci.* **52**, 225–232 (1990).
28. Tirnauer, J. S., Salmon, E. D. & Mitchison, T. J. Microtubule plus-end dynamics in *Xenopus* egg extract spindles. *Mol. Biol. Cell* **15**, 1776–1784 (2004).
29. Lin, W., Ame, J. C., Aboul-Ela, N., Jacobson, E. L. & Jacobson, M. K. Isolation and characterization of the cDNA encoding bovine poly(ADP-ribose) glycohydrolase. *J. Biol. Chem.* **272**, 11895–11901 (1997).

Supplementary Information accompanies the paper on www.nature.com/nature.

Acknowledgements We thank A. Pollington, B. Ward, J. Tirnauer and B. Briehier for critical reading of the manuscript; A. Straight for CENPE antibodies; A. Groen and D. Miyamoto for TPX2, NuMA and Eg5 antibodies; Z. Perlman for assistance with data analysis; D. L. Coyle for technical support; and the Nikon Imaging Facility at Harvard Medical School for use of microscopes. This work was supported by NIH grants to T.M.J. and M.K.J.

Competing interests statement The authors declare that they have no competing financial interests.

Correspondence and requests for materials should be addressed to P.C. (paul_chang2@hms.harvard.edu).

Structure of an auxilin-bound clathrin coat and its implications for the mechanism of uncoating

Alexander Fotin¹, Yifan Cheng², Nikolaus Grigorieff³, Thomas Walz², Stephen C. Harrison⁴ & Tomas Kirchhausen⁵

¹Biophysics Graduate Program, ²Department of Cell Biology, Harvard Medical School, 240 Longwood Avenue, Boston, Massachusetts 02115, USA
³Howard Hughes Medical Institute and Department of Biochemistry, Rosenstiel Basic Medical Sciences Research Center, Brandeis University, 415 South Street, Waltham, Massachusetts 02454, USA
⁴Department of Biological Chemistry and Molecular Pharmacology, Harvard Medical School, and Howard Hughes Medical Institute, 250 Longwood Avenue, Boston, Massachusetts 02115, USA
⁵Department of Cell Biology and the CBR Institute for Biomedical Research, Harvard Medical School, 200 Longwood Avenue, Boston, Massachusetts 02115, USA

Clathrin-coated pits invaginate from specific membrane compartments and pinch off as coated vesicles. These vesicles then uncoat rapidly once released. The Hsc70 molecular chaperone effects the uncoating reaction, and is guided to appropriate locations on clathrin lattices by the J-domain-containing co-chaperone molecule auxilin^{1–4}. This raises the question of how a local event such as ATP hydrolysis by Hsc70 can catalyse a global disassembly. Here, we have used electron cryomicroscopy to determine 12-Å-resolution structures of *in-vitro*-assembled clathrin coats in association with a carboxy-terminal fragment of auxilin that contains both the clathrin-binding region and the J domain. We have located the auxilin fragment by computing differences between these structures and those lacking auxilin (described in an accompanying paper⁵). Auxilin binds within the clathrin lattice near contacts between an inward-projecting C-terminal helical tripod and the crossing of two ‘ankle’ segments; it also contacts the terminal domain of yet another clathrin ‘leg’. It therefore recruits Hsc70 to the neighbourhood of a set of critical interactions. Auxilin binding produces a local